

Colloidal co-assembly route to large-area, high-quality photonic crystals

Lidiya Mishchenko¹, Benjamin Hatton¹, Ian B. Burgess¹, Stan Davis², Kenneth Sandhage², Joanna Aizenberg¹

[1] School of Engineering and Applied Sciences, Harvard University, Cambridge MA
[2] School of Materials Science and Engineering, Georgia Institute of Technology, Atlanta GA

ABSTRACT

Whereas considerable interest exists in self-assembly of well-ordered, porous "inverse opal" structures for optical, electronic, and (bio)chemical applications, uncontrolled defect formation has limited the scale-up and practicality of such approaches. Here we demonstrate a new method for assembling highly ordered, crack-free inverse opal films over a centimeter scale. Multilayered composite colloidal crystal films have been generated via evaporative deposition of polymeric colloidal spheres suspended within a hydrolyzed silicate sol-gel precursor solution. The co-assembly of a sacrificial colloidal template with a matrix material avoids the need for liquid infiltration into the preassembled colloidal crystal and minimizes the associated cracking and inhomogeneities of the resulting inverse opal films. We demonstrate that this co-assembly approach allows the fabrication of hierarchical structures not achievable by conventional methods, such as multilayered films and deposition onto patterned or curved surfaces, and can be transformed into various materials that retain the morphology and order of the original films. We show that colloidal co-assembly represents a simple, low-cost, scalable method for generating high-quality, chemically tailorable inverse opal films for optical applications.

Keywords: colloid, self-assembly, inverse opal, photonic crystal, silica, silicon, conversion, hierarchical

INTRODUCTION

Self-assembly methods have proven to be undeniably important for the synthesis of nanoporous solids impossible by conventional top-down methods. Nanoporous inorganic networks have been synthesized using a variety of self-assembled organic templates. Examples include self-assembled supramolecular and colloidal templates to direct the structure of sol-gel oxide precursors, to produce mesoporous and 'inverse opal' materials¹⁻⁶. Inverse opal structures combine a high degree of interconnected porosity (~ 75%), with highly-uniform pore size (achieved through colloidal size monodispersity). Such ordered, high surface area, nanoporous networks are important for a range of useful applications in fields from catalysis to tissue engineering, drug delivery, gas sensing, filtration and photonics⁷⁻¹⁰. In particular, periodic inverse opal structures have been demonstrated to have 3D photonic band gaps, with sufficient refractive index contrast^{6, 11-12}. Also, the static and dynamic control of the bright reflected colors in low-refractive-index materials ($n \sim 1.5$) is desirable in applications such as low-power displays, structural papers and inks, and chemical sensors¹³⁻¹⁶. However, the control of defects remains a persistent problem associated with bottom-up self-assembly, compared to conventional top-down methods fabrication.

The conventional synthesis of inverse opal materials involves the infiltration of a matrix material around a sacrificial template *after* its self-assembly^{2-3, 6, 10, 12}, as illustrated in **Figure 1a**, before removal of the template. Colloidal crystals templates can be produced by methods such as sedimentation¹, shear flow⁴, and evaporative¹⁷⁻¹⁹ or 'flow controlled' deposition²⁰⁻²¹ of films on a substrate. Colloidal crystal assembly (such as PS or PMMA) as a template is typically followed by infiltration of a sol-gel solution (2), before removing the template (3) to produce an inverse inorganic porous structure. This method has been used for a wide range of inverse opals, such as SiO₂, TiO₂, and Al₂O₃,

using solution sol-gel precursors such as metal alkoxides^{1,4}, the infiltration of nanoparticles²⁰, or by deposition from a vapor phase^{11, 22-23}.

This conventional infiltration method does produce highly-ordered structures at small scales, but produces a number of defects such as cracks, domain boundaries and overlayer coatings at larger length scales². For the formation of inverse opal films it is generally difficult to achieve structural uniformity over length scales beyond ~50 µm due to under- or over-infiltration, which causes either structural collapse and cracking, or overlayer formation. Cracking also often results due to the high capillary forces associated with the infiltration of a liquid into the high-curvature pores of the fragile colloidal crystal. Vapor phase deposition (ALD) avoids the problems of liquid infiltration, but is time consuming and expensive^{11, 22-23}. Some efforts have been made to increase the strength of the template using partial sintering of the colloidal crystal²⁴, the growth of necks between spheres²⁵⁻²⁶, or to use a more gentle method of sol-gel infiltration²¹. In addition, efforts have been made to control the cracking²⁷ and domain orientation of colloidal crystal films through control of the evaporative deposition conditions^{19, 28}, pre-sintering of the particles²⁹, and deposition onto topologically-patterned substrates³⁰. Ultimately, however, there have been no reliable methods to produce inverse opal films that are crack-free and with large domains over significantly large areas.

Herein, we have developed a simplified one-step, co-assembly process to combine the colloidal and sol-gel self-assembly using evaporative deposition to produce highly-ordered inverse opal films over large areas **Figure 1b**. The evaporative deposition of colloidal crystal films involves a vertically-oriented substrate that allows the self-assembly of the colloidal particles at the meniscus^{17-18, 31}. The evaporative co-assembly method involves the deposition of polymer colloidal particles with a silica sol-gel addition, to produce a SiO₂ matrix distributed in the interstitial space of the PMMA particles. Previously Wang *et al*³² added tetraethoxysilane (TEOS) to a SiO₂ colloidal suspension to form SiO₂ necks between spheres as a means of reducing cracking, though the necks were later etched away. Otherwise there has been no previous account of colloidal self-assembly directly with sol-gel precursors in solution.

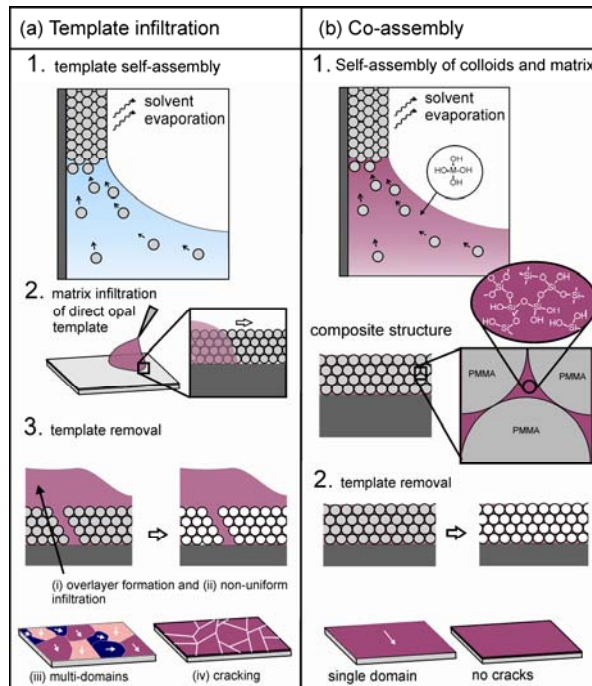


Figure 1. Schematics of ‘conventional’ colloidal template self-assembly (a), and co-assembly of colloids with a soluble matrix precursor (b), for the syntheses of inverse opal thin films. The conventional method typically involves the sequential steps of colloidal self-assembly, matrix infiltration, and template removal. The use of such conventional colloidal self-assembly to generate large-area films has been plagued with the formation of defects, such as overlayer coatings, multiple domains, and significant cracking. Colloidal co-assembly combines the steps of template self-assembly with matrix infiltration into one process in which colloids are allowed to assemble directly from the sol-gel solution, to yield robust inverse opal films with no overlayer, very large (*mm* to *cm*) ordered domains, and no cracks, due to the “gluing” action of the sol-gel matrix.

EXPERIMENT

Colloidal particles of PMMA or PS were synthesized by emulsion polymerization, using an ammonium persulfate initiator, or purchased commercially (IFC Invitrogen). A glass or Si substrate, $\sim 1 \times 4$ cm and cleaned in piranha solution, was vertically suspended in a vial containing a 20 mL volume of 0.5 – 3.0 vol% colloidal suspensions. The suspensions contained X mL of added hydrolyzed TEOS solution, where X was varied from 0 to 0.50 mL. The TEOS solution consisted of 1:1:1.5 ratio by weight of TEOS (98% Aldrich), 0.10 M HCl, and EtOH (100%), respectively, stirred at room temperature for 1 h prior to use. The colloidal/TEOS suspension was allowed to evaporate slowly over a period of 1-3 days in a 65°C oven on a pneumatic vibration-free table, to allow the deposition of a thin film onto the suspended substrate. The films were calcined in air at 500°C for 5 h, with a 4 h ramp time (Thermo Scientific).

Reactive (magnesiothermic) conversion of the I-SiO₂ films into Si/MgO was achieved by sealing an I-SiO₂ film on Si wafer with a solid Mg vapor source (Alfa Aesar, Ward Hill, MA), inside a steel ampoule, in an Ar atmosphere³³. The ampoule was heated at a rate of 5°C/min to 850°C and held at this temperature for 4 h to allow for conversion of the I-SiO₂ film into a Si/MgO composite film. After cooling and removal from the steel ampoule, the reacted film was immersed in a stirred 0.10 M HCl solution at 70°C for 3 h in order to selectively dissolve the MgO product to yield a porous Si inverse opal film.

Optical spectra were taken using a microscope-based fiber optic spectrometer system (Ocean Optics USB2000+, 300-800 nm range) on a Leica DMRX microscope using a 10x objective. Film structures were imaged by SEM (Zeiss Ultra) at 10 kV after Pt/Pd-sputter coating and by TEM (JEOL 2100) at 200 kV on fragments of the films deposited onto Formvar-coated Cu grids (EMS).

RESULTS

Co-Assembly

Figure 2 compares the quality of the co-assembled inverse SiO₂ films with the PMMA colloidal crystals and inverse SiO₂ films generated by infiltration, of approximately the same thickness. A typical PMMA colloidal crystal deposited by evaporative deposition (from a solution containing no TEOS), shows significant cracking (**Figure 2a**). A variety of defects and micron-sized misaligned domains are evident. The infiltration step further reduced the quality of the films due to the formation of an overlayer, partial filling of the cracks developed during the assembly of the template PMMA crystal, and an additional ‘glassy’ crack pattern originated from the overlayer and non-uniform infiltration (**Figure 2b**). The co-assembled inverse SiO₂ film (**Figure 2c-d**) was produced under the following optimized conditions: i) suspending a vertically-oriented glass slide in a mixture comprised of 0.15 mL of a 28.6 wt% TEOS solution with a 20 mL suspension of 280 nm diameter PMMA spheres (~0.125 vol%), ii) allowing the solvent to slowly evaporate at 65°C (deposition rate = 2 cm/day), and iii) treating the deposited film at 500°C for 5 h in air. These conditions were found to generate nearly perfect, crack-free inverse opal films. The colloidal volume fraction (for constant TEOS/PMMA ratio) determines the thickness of the films, which varies linearly with concentration.

In general, the TEOS/colloid ratio controls the film structure and defects. Insufficient silicate additions do not allow the formation of a continuous SiO₂ network around the colloidal template, which causes significant cracking (ie; ‘tearing’). The SiO₂ additions appear to act as a ‘glue’, and at a critical amount of the TEOS addition, there is sufficient SiO₂ matrix to allow the formation of highly-ordered, crack-free films. Cracking of opal and inverse opal films often occurs upon drying due to a combination of dehydration, polymerization-induced contraction, and local capillary forces^{27,34}. Colloidal crystal films constrained on fixed substrate are generally too weak to resist such tensile stresses, but the composite silica-colloid structure formed via co-assembly is better able to withstand these conditions.

The film in **Figure 2c-d** is a highly-uniform, crack-free film from the co-assembly of 280 nm PMMA spheres (vertical deposition direction, from top to bottom). **Figure 2e** shows an optical picture of the film showing the distinct, uniform color due to the optical interference. **Figure 2e** also shows the optical spectrum of the SiO₂ inverse opal film, measured in reflectance, showing a well-defined Bragg peak at around 480 nm. The position of this first stop gap (λ_{111}) for the {111} planes, can be found to be at the given wavelength:

$$\lambda_{(111)} = 2 \cdot d_{(111)} \cdot \sqrt{\langle \epsilon \rangle - \sin^2 \theta} \quad [1]$$

where $d_{(111)}$ is the d-spacing of the {111} planes, θ is the incidence angle, and $\langle \epsilon \rangle$ is the volume averaged dielectric constant of the composite, given by,

$$\langle \epsilon \rangle = V_{SiO_2} \cdot \epsilon_s + (1 - V_{SiO_2}) \cdot \epsilon_b \quad [2]$$

where V_{SiO_2} is the filling fraction of silica, and ϵ_s and ϵ_b the dielectric constant of the spheres and the background, respectively.

Another important aspect of co-assembled inverse opals is that these films have no overlayer coating at the ideal ratio. (Although increasing the TEOS content in the suspensions beyond the ideal ratio (ie; the films in Figure 2c-d) causes the initial formation of an overlayer, which continues to thicken with larger TEOS additions.) That means that the extremely high porosity of the films is entirely accessible from the top surface. This property of the films is very important for applications such as catalysis, gas adsorption, or tissue engineering, and is not easily achieved using conventional infiltration methods^{1-2, 5}.

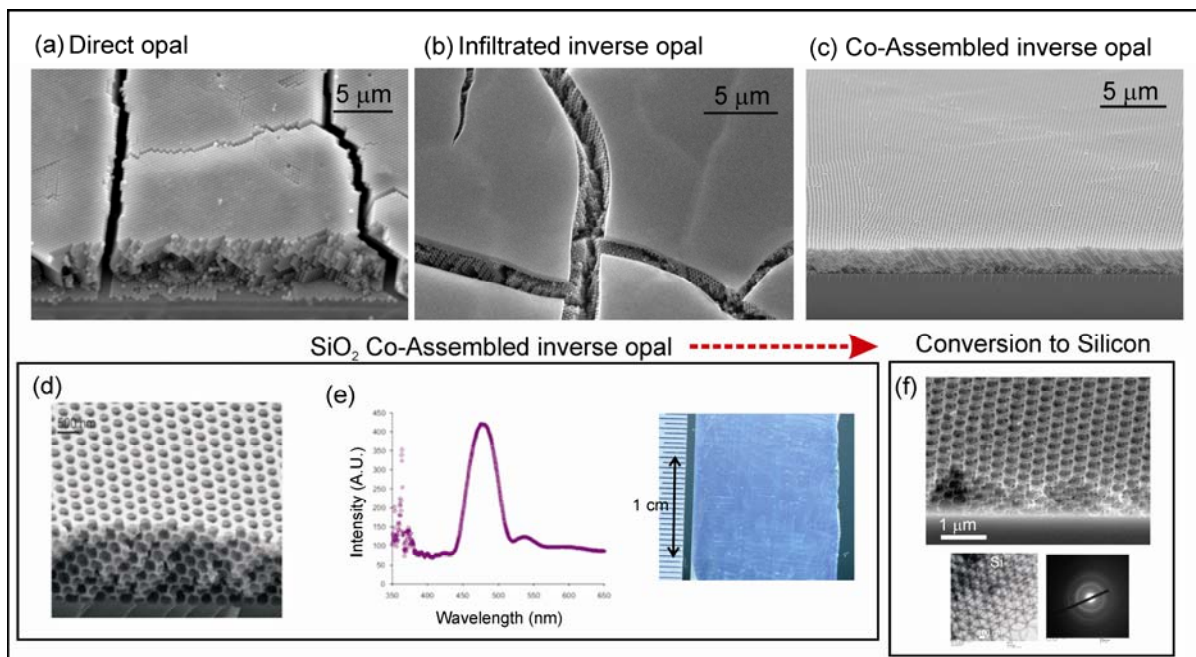


Figure 2. SEM images of colloidal and inverse opal films and morphology-preserving reactive transformation of inverse opal SiO_2 films into Si. (a) PMMA colloidal crystal film (as-synthesized), showing cracks; (b) inverse opal SiO_2 film formed by sol-gel infiltration (calcined to remove PMMA template), showing an overlayer coating, cracking in both the inverse opal and overlayer coating; (c-d) inverse opal film formed by PMMA/sol-gel co-assembly (calcined), showing highly-uniform films with no cracks. An optical image and reflectance spectrum of the co-assembled inverse opal are shown in (e). SEM and TEM images with SAED analysis are shown for a Si inverse opal film (f) after transformation of the silica opal.

Conversion

The conversion of co-assembled inverse SiO_2 films into Si inverse opals was conducted via a ‘magnesiothermic’ reaction with Mg vapor to generate a co-continuous Si/MgO nanocomposite³³. The MgO phase was then selectively removed to produce a highly-porous Si structure. SEM and TEM analyses of the final Si-converted structure are shown in **Figures 2f**. The Si/MgO -converted film retained a highly periodic structure, and no additional cracks formed throughout the converted film. The Si/MgO -composite exhibited a modest (~10%) contraction in the direction normal to the film, relative to the starting I- SiO_2 film, however. The selected area electron diffraction (SAED) pattern in **Figure 2f**

confirms the presence of Si, although small amounts of residual (undissolved) Mg and O were detected by EDS. High resolution TEM imaging indicated that the Si inverse opal films are composed of 5-10 nm nanocrystals.

Hierarchical Structures

The direct combination of the colloidal template and matrix gives this method a great versatility for the fabrication of inverse opal layers in structures and applications not practically possible by conventional methods. **Figure 3** shows representative examples of such complex, hierarchical materials. Multilayer inverse opal structures with varying pore sizes can be created by the successive deposition of template/matrix composite layers (**Figure 3a**). Such structures could have important applications in differential drug release, where sequential dosed release of components can be achieved by selective pore size engineering due to the differences in the rate of desorption and diffusion. **Figure 3b** reveals patterned inverse opal deposited within channel structures on a Si substrate. There is a structural hierarchy associated with these structures, at the colloidal and micrometer scales, which can be used to engineer the colloidal assembly. Finally, co-assembly can be used to deposit inverse opals onto arbitrarily-shaped substrates, such as curved surfaces. **Figure 3c** shows Ti beads coated with an inverse opal layer. Such high-surface area, hierarchical assemblies could have important applications for catalysis and biomedical surfaces.

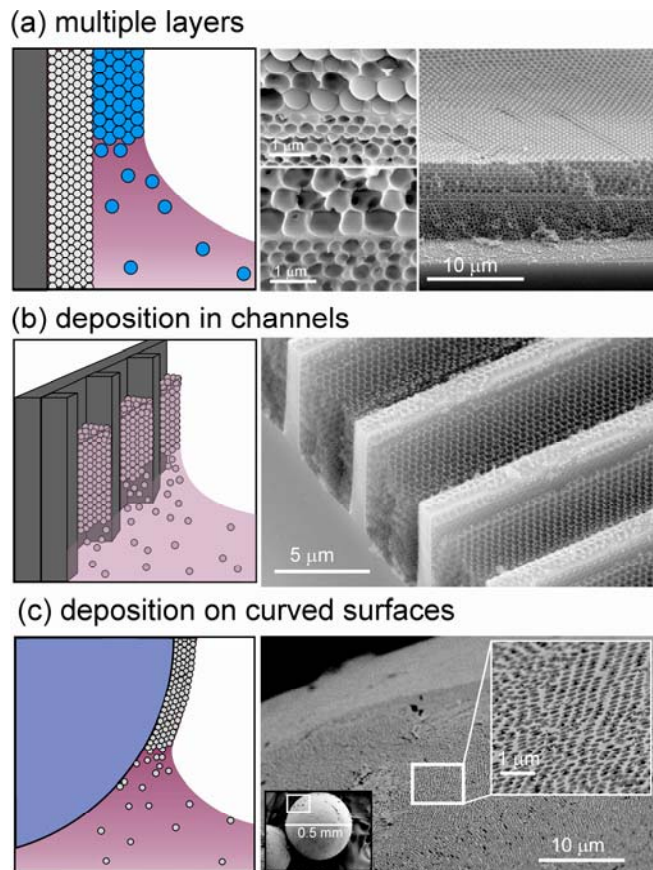


Figure 3. Novel SiO_2 inverse opal structures enabled by colloidal co-assembly. Schematics of the processes are shown on the left and the representative SEM images are shown on the right. (a) Schematic presentation of the synthesis of multi-layered, hierarchical films with different pore sizes by successive layer deposition prior to template removal (left), and a SEM cross-section images of a bi-layer SiO_2 structure produced using 300 nm and 720 nm colloidal spheres (right). The top left and bottom left SEM images show the interface between layers before and after calcination, respectively. (b) Schematic presentation of the oriented SiO_2 structures grown on topologically-patterned blade substrates (left), and an SEM fractured cross-section of inverse opals grown in 4 μm wide, 5 μm deep channels on a Si substrate (right). (c) Schematic presentation of the co-assembly onto curved surfaces (left), and SEM images (right) of a SiO_2 inverse opal film layer (shown magnified, inset) deposited onto a sintered, macroporous Ti scaffold structure.

The deposition of inverse opals into geometrically patterned surfaces (as seen in Figure 3b) can also be used to change the optical properties of colloidal crystals. Preliminary results with direct colloidal crystals show that the order and cracking of films can be controlled by deposition into post (**Figure 4a**) and channel (**Figure 4b**) structures of different widths and spacings. These concepts can be easily extended to co-assembled inverse opals and could allow for the assembly of discrete optical elements or patterned optical circuits.

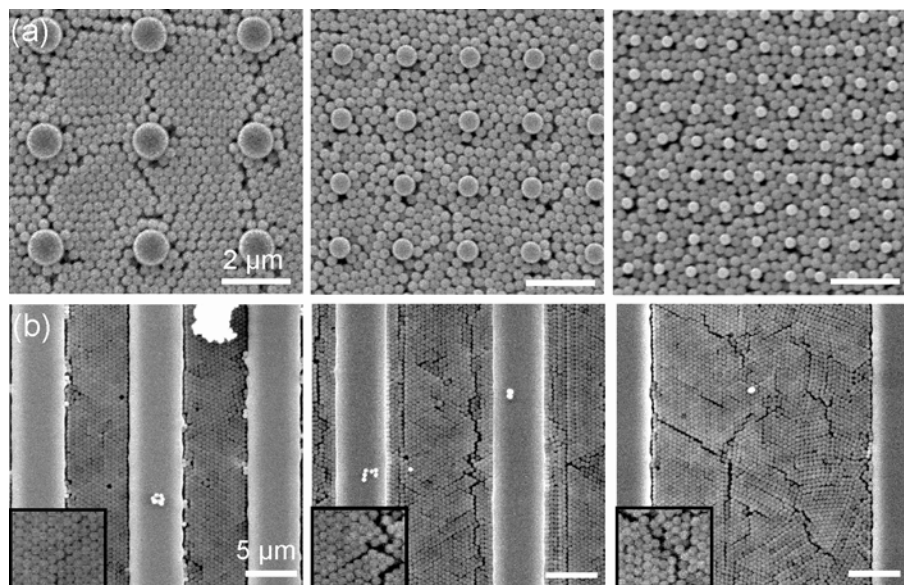


Figure 4. Exploring hierarchical colloidal assembly. Direct colloidal assembly of colloids into 2 μm tall post (a) and blade/channel (b) SU8 structures of various feature sizes and spacings.

CONCLUSIONS

In summary, we have demonstrated the first synthesis of crack-free, highly-ordered inverse opal films over *cm* length scales by a simple two-step, solution-based colloidal/matrix co-assembly process. Major advantages of this co-assembly process include: (1) a great reduction in the defect population (particularly crack density), (2) the growth of large, highly-ordered domains via a scalable process, (3) prevention of overlayer formation and non-uniform infiltration, and (4) minimizing the number of fabrication steps (i.e., avoidance of post-assembly infiltration provides a time/cost/quality advantage), (5) the ability to form multilayered, hierarchical, patterned and curved film structures that are not easily possible by any other method. Furthermore, we have demonstrated that these SiO_2 inverse opal films are sufficiently robust and homogeneous to allow direct conversion, via morphology-preserving gas/solid displacement reactions, into inverse opal films comprised of other materials, such as porous Si. The unusual crystallographic orientation and crack patterns observed in these films also pose interesting fundamental questions in soft condensed matter and fracture mechanics. This scalable route to highly-ordered, large area, chemically-tailorable inverse opal films may be utilized in a diverse range of applications, including photonics¹⁶, catalysis³⁵, tissue engineering³⁶, gas adsorption³⁷ and sensing¹⁶.

ACKNOWLEDGEMENTS

This project was supported by the Office of Naval Research under Award N00014-07-1-0690-DOD35CAP and by the Air Force Office of Scientific Research under Award FA9550-09-1-0669-DOD35CAP. The work was performed in part

at the Center for Nanoscale Systems (CNS), a member of the National Nanotechnology Infrastructure Network (NNIN), which is supported by the National Science Foundation under Award ECS-0335765. L.M. thanks the US Department of Homeland Security (DHS) for the fellowship. The DHS Scholarship and Fellowship Program is administered by the Oak Ridge Institute for Science and Education (ORISE) through an interagency agreement between the US Department of Energy (DOE) and DHS. ORISE is managed by Oak Ridge Associated Universities (ORAU) under DOE Contract DE-AC05-06OR23100.

REFERENCES

1. Holland, B. T.; Blanford, C. F.; Stein, A., "Synthesis of Macroporous Minerals with Highly Ordered Three-Dimensional Arrays of Spheroidal Voids", *Science* 281, 538 (1998).
2. Lytle, J. C.; Stein, A., "Recent Progress in Synthesis and Applications of Inverse Opals and Related Macroporous Materials Prepared by Colloidal Crystal Templating", *Ann. Rev. Nano Res.* 1, 1 (2006).
3. Stein, A.; Schrodin, R. C., "Colloidal Crystal Templating of Three-Dimensional Ordered Macroporous Solids: Materials for Photonics and Beyond", *Current Opinion in Solid State and Materials Science* 5, 553 (2001).
4. Velev, O. D.; Jede, T. A.; Lobo, R. F.; Lenhoff, A. M., "Porous Silica Via Colloidal Crystallization", *Nature* 389, 447 (1997).
5. Velev, O. D.; Lenhoff, A. M., "Colloidal Crystals as Templates for Porous Materials", *Current Opinion in Colloid and Interface Science* 5, 56 (2000).
6. Xia, Y.; Gates, B.; Yin, Y.; Lu, Y., "Monodispersed Colloidal Spheres: Old Materials with New Applications", *Adv. Mater.* 12, 693 (2000).
7. Davis, M. E., "Ordered Porous Materials for Emerging Applications.", *Nature* 417, 813 (2002).
8. Gibson, L. J.; Ashby, M. F., [Cellular Solids], Cambridge University Press, Cambridge, UK, (1997).
9. Yaghi, O. M.; Li, H. L.; Davis, C.; Richardson, D.; Groy, T. L., "Synthetic Strategies, Structure Patterns, and Emerging Properties in the Chemistry of Modular Porous Solids", *Acc. Chem. Res.* 31, 474 (1998).
10. Zhao, X. S.; Su, F. B.; Yan, Q. F.; Guo, W. P.; Bao, X. Y.; Lv, L.; Zhou, Z. C., "Templating Methods for Preparation of Porous Structures", *J. Mater. Chem.* 16, 637 (2006).
11. Blanco, A.; Chomski, E.; Graptchak, S.; Ibisate, M.; John, S.; Leonard, S. W.; Lopez, C.; Meseguer, F.; Miguez, H.; Mondia, J. P.; Ozin, G. A.; Toader, O.; van Driel, H. M., "Large-Scale Synthesis of a Silicon Photonic Crystal with a Complete Three-Dimensional Bandgap near 1.5 Micrometres", *Nature* 405, 437 (2000).
12. Colvin, V. L., "From Opals to Optics: Colloidal Photonic Crystals", *MRS Bulletin* 26, 637 (2001).
13. Aguirre, C. I.; Reguera, E.; Stein, A., "Tunable Colors in Opals and Inverse Opal Photonic Crystals", *Adv. Funct. Mater.* 20, 2565 (2010).
14. Schrodin, R. C.; Al-Daous, M.; Blanford, C. F.; Stein, A., "Optical Properties of Inverse Opal Photonic Crystals", *Chem. Mater.* 14, 3305 (2002).
15. Arsenault, A. C.; Puzzo, D. P.; Manners, I.; Ozin, G. A., "Photonic-Crystal Full-Colour Displays", *Nat. Photonics* 1, 468 (2007).
16. Arsenault, A. C.; Clark, T. J.; Von Freymann, G.; Cademartiri, L.; Sapienza, R.; Bertolotti, J.; Vekris, E.; Wong, S.; Kitaev, V.; Manners, I.; Wang, R. Z.; John, S.; Wiersma, D.; Ozin, G. A., "From Colour Fingerprinting to the Control of Photoluminescence in Elastic Photonic Crystals", *Nat. Mater.* 5, 179 (2006).
17. Dimitrov, A. S.; Nagayama, K., "Continuous Convective Assembling of Fine Particles into Two-Dimensional Arrays on Solid Surfaces", *Langmuir* 12, 1303 (1996).
18. Jiang, P.; Bertone, J. F.; Hwang, K. S.; Colvin, V. L., "Single-Crystal Colloidal Multilayers of Controlled Thickness", *Chem. Mater.* 11, 2132 (1999).
19. Wong, S.; Kitaev, V.; Ozin, G. A., "Colloidal Crystal Films: Advances in Universality and Perfection", *J. Am. Chem. Soc.* 125, 15589 (2003).
20. Gu, Z.; Fujishima, A.; Sato, O., "Fabrication of High-Quality Opal Films with Controllable Thickness", *Chem. Mater.* 14, 760 (2002).
21. Zhou, Z. C.; Zhao, X. S., "Opal and Inverse Opal Fabricated with a Flow-Controlled Vertical Deposition Method", *Langmuir* 21, 4717 (2005).

22. King, J. S.; Heineman, D.; Graungnard, E.; Summers, C. J., "Atomic Layer Deposition in Porous Structures: 3d Photonic Crystals", *Appl. Surf. Sci.* 244, 511 (2005).
23. Scharrer, M.; Wu, X.; Yamilov, A.; Cao, H.; Chang, R. P. H., "Fabrication of Inverted Opal ZnO Photonic Crystals by Atomic Layer Deposition", *Appl. Phys. Lett.* 86, 151113 (2005).
24. Míguez, H.; Meseguer, F.; López, C.; Blanco, A.; Moya, J. S.; Requena, J.; Mifsud, A.; Fornés, V., "Control of the Photonic Crystal Properties of Fcc Packed Submicron SiO₂ Spheres by Sintering", *Adv. Mater.* 10, 480 (1998).
25. Miguez, H.; Tetreault, N.; Hatton, B. D.; Yang, S. M.; Perovic, D. D.; Ozin, G. A., "Mechanical Stability Enhancement by Pore Size and Connectivity Control in Colloidal Crystals by Layer-by-Layer Growth of Oxide", *Chem. Comm.*, 2736 (2002).
26. Wang, L.; Zhao, X. S., "Fabrication of Crack-Free Colloidal Crystals Using a Modified Vertical Deposition Method", *J. Phys. Chem. C* 111, 8538 (2007).
27. Tirumkudulu, M. S.; Russel, W. B., "Cracking in Drying Latex Films", *Langmuir* 21, 4938 (2005).
28. McLachlan, M. A.; Johnson, N. P.; De La Rue, R. M.; McComb, D. W., "Thin Film Photonic Crystals: Synthesis and Characterisation", *J. Mater. Chem.* 14, 144 (2004).
29. Chabanov, A. A.; Jun, Y.; Norris, D. J., "Avoiding Cracks in Self-Assembled Photonic Band-Gap Crystals", *Appl. Phys. Lett.* 84, 3573 (2004).
30. Dziomkina, N. V.; Vancso, G. J., "Colloidal Crystal Assembly on Topologically Patterned Templates", *Soft Matter* 1, 265 (2005).
31. Norris, D. J.; Arlinghaus, E. G.; Meng, L.; Heiny, R.; Scriven, L. E., "Opaline Photonic Crystals: How Does Self-Assembly Work?", *Adv. Mater.* 16, 1393 (2004).
32. Wang, L.; Zhao, X. S., "Fabrication of Crack-Free Colloidal Crystals Using a Modified Vertical Deposition Method", *J. Phys. Chem. C* 111, 8538 (2007).
33. Bao, Z. H.; Weatherspoon, M. R.; Shian, S.; Cai, Y.; Graham, P. D.; Allan, S. M.; Ahmad, G.; Dickerson, M. B.; Church, B. C.; Kang, Z. T.; Abernathy, H. W.; Summers, C. J.; Liu, M. L.; Sandhage, K. H., "Chemical Reduction of Three-Dimensional Silica Micro-Assemblies into Microporous Silicon Replicas", *Nature* 446, 172 (2007).
34. Brinker, C. J.; Scherer, G. W., [Sol-Gel Science: The Physics and Chemistry of Sol-Gel Processing.], Academic, (1990).
35. Guan, G. Q.; Zapf, R.; Kolb, G.; Hessel, V.; Lowe, H.; Ye, J. H.; Zentel, R., "Preferential Co Oxidation over Catalysts with Well-Defined Inverse Opal Structure in Microchannels", *Int. J. Hydrogen Energy* 33, 797 (2008).
36. Choi, S. W.; Xie, J. W.; Xia, Y. N., "Chitosan-Based Inverse Opals: Three-Dimensional Scaffolds with Uniform Pore Structures for Cell Culture", *Adv. Mater.* 21, 2997 (2009).
37. Kang, S.; Yu, J. S.; Kruk, M.; Jaroniec, M., "Synthesis of an Ordered Macroporous Carbon with 62 Nm Spherical Pores That Exhibit Unique Gas Adsorption Properties", *Chem. Commun. (Cambridge, U. K.)*, 1670 (2002).